Pure hydrogen co-production by membrane technology in an IGCC power plant with carbon capture

Aristide Giuliano, Massimo Poletto, Diego Barletta*

Dipartimento di Ingegneria Industriale, Università degli Studi di Salerno

Via Giovanni Paolo II, 132, 84084 Fisciano (SA), Italy

Abstract

The CO_2 capture in Integrated Gasification Combined Cycle (IGCC) plants causes a significant increase of the cost of electricity (COE) and thus determines high CO_2 mitigation cost (cost per ton of avoided CO_2 emissions). In this work the economic sustainability of the co-production of pure hydrogen in addition to the electricity production was assessed by detailed process simulations and a techno-economic analysis. To produce pure hydrogen a Water Gas Shift reactor and a Selexol® process was combined withH_2 selective palladium membranes. This innovative process section was compared with the more conventional Pressure Swing Adsorption in order to produce amount of pure hydrogen up to 20% of the total hydrogen available in the syngas.

Assuming for a base case a hydrogen selling price of 3 €/kg and a palladium membrane cost of 9200 €/m^2, a cost of energy (COE) of 64 €/MWh and a mitigation cost of 20 €/ton_{CO2} were obtained for 90% captured CO_2 and 10% hydrogen recovery. An increase of the hydrogen recovery up to 20% determines a reduction of the COE and of the mitigation cost to 50 €/MWh and 5 €/ton_{CO2}, respectively. A sensitivity analysis showed that even a 50% increase of cost of the membrane per unit surface could determine a COE increase of only about 10% and a maximum increase of the mitigation cost of further 5 €/ton_{CO2}.

Keywords: IGCC, carbon capture, hydrogen, mitigation cost, palladium membrane, PSA.

* corresponding author Tel: +39 089 962499; Fax: +39 089 968 781; E: dbarletta@unisa.it

https://doi.org/10.1016/j.ijhydene.2018.08.112

1 Introduction

According to the IPCC report of 2014 [1], global warming of more than 2 °C could have serious consequences, such as the substantial increase in the number of extreme climatic events. The major cause of global warming is the increase of carbon dioxide in the atmosphere. Carbon pricing mechanisms, either cap and trade systems or carbon tax, already adopted by about 40 countries, can be effective political tools in order to aim at the greenhouse gas emissions reduction according to the 2015 Paris agreement [2].

In recent years, coal is still a significant source of energy for economic and geopolitical reasons. In this scenario, the so-called Clean Coal Technologies (CCT) have been developed to aim at extracting, treating and using coal in an efficient manner and with a reduced environmental impact.

The Integrated Gasification Combined Cycle (IGCC) is a well established technology to produce electricity through a Combined Cycle Unit (CCU) from low calorific fuel gas obtained by gasification of coal, refinery petcoke, and other residues [3]. In addition to electricity generation, IGCC allows the co-production of hydrogen and steam. The IGCC has promising potentialities to apply pre-combustion CO_2 capture technologies[4]. In fact, the CO_2 in the clean syngas is available at high pressure, which makes the capture easier and significantly reduces the compression costs for final storage. [5]. However, the addition of a carbon capture and storage (CCS) section causes a significant loss of net produced energy corresponding to a reduction of efficiency, the so called energy penalty, up to ten points [6]. Optimized process schemes were also proposed to reduce these efficiency losses [7]. In particular, this depends on a net loss of the mass flow rate of the gas through the gas turbines, and on a further reduction of efficiency due to the presence of a water-gas shift stage [8]. Moreover, according to the estimates by Cormos [6], there is a 22.5% increase in investment costs to carry out a 90% CCS capture.The resulting Cost of Energy (COE) with CCS increases up to more than 90 €/MWhe [9]

In order to mitigate the economic disadvantages of the carbon capture, it is possible to implement the co-production of pure hydrogen that has a high added value and can be used for both energy and industrial uses [10].

Pressure Swing Adsorption (PSA) is a common hydrogen separation technology for large-scale separations due to its technical simplicity and low operating costs [11]. The conventional process solution is, thus, given by a water gas shift stage to enrich the syngas in H_2 and CO_2, followed by a PSA section to separate the hydrogen [12]. Process simulation results by Riboldi & Bolland [11] showed that it is possible to significantly change the relative amounts of electricity and hydrogen with acceptable global plant efficiency, including the pure hydrogen stream.

More recently, extensive research work has been performed to develop highly selective metal membranes to obtain hydrogen with purity larger than 99% [13]. Process integration and reaction enhancement were pursued by several studies proposing the WGS catalytic reactor and the hydrogen selective membranes occuring in a single unit named water gas shift membrane reactor (WGSMR) [14,15]. An alternative promising technology for both electricity and hydrogen production from gasification with CO_2 capture is provided by Syngas Chemical Looping (SCL) [16]. More recent developments aim at an integration of gasification and chemical looping by the so-called Coal Direct Chemical Looping (CDCL) [17,18], with the chemical storage by methylcyclohexane (MCH) and/or coupling with Solid Oxide Fuel Cells (SOFC) [19].

A comparative preliminary techno-economic analysis by Li et al. [20] revealed that both WGS coupled with membrane technology and SCL technology are competitive for electricity and hydrogen production with 90% CO_2 capture. However, the economic figures of this study might be approximate since detailed sizing of main process units was not addressed. Some techno-economic studies addressed the integration of Pd-based H_2-selective membranes in a IGCC plant, but for power generation only [21–23]. Techno-economic analysis with investment cost estimate based on accurate sizing of the additional process equipment to co-produce hydrogen by membrane technology is lacking in the literature.

The aim of this work is to provide a technical and economic analysis of an IGCC process with up to date carbon capture technologies and with co-production of electricity and high purity molecular hydrogen in order to mitigate the capture costs of CO_2. The most promising alternative processes at the industrial scale are selected and included in the possible flowsheet to separate H_2 and CO_2. In particular, innovative palladium-based membranes are considered for the co-production of pure H_2, while absorption with the Selexol® solvent is assessed for carbon capture. The latter process sections are optimized from a technical and economic standpoint of view and compared with the traditional sequence of Selexol® process and Pressure Swing Adsorption (PSA). Detailed unit sizing of the new process section is performed by rigouros design methods available in process simulation software.

With concern to the economic analysis, investment and operational costs for the capture and storage of CO_2 and pure H_2 production, and consequently of the entire IGCC power plant were calculated. The ultimate aim was to define two macroscopic indexes, the production cost of energy and the mitigation cost of the carbon capture, to assess the alternative process technologies for different values of the CO_2 capture percentage. Finally, sensitivity analysis on the Pd membrane cost is also performed to take into account the cost uncertainty of developing technologies.

2 Process simulation

2.1 Case study description

In this work the section of CO_2 capture and H_2 production of an IGCC power plant was simulated. The inlet stream to this section was the syngas stream, mainly formed by CO and H_2, coming out of the gas cleaning section of an IGCC plant. In particular, in this case study we referred to the clean syngas stream generated from a solid 50:50 mixture of petroleum coke and coal in the 335MWe Puertollano IGCC power plant according to the data simulated and reported by Sofia et al. [24,25]. The stream composition and operating conditions are reported in Table 1.

Table 1: Composition and conditions of clean gas flowrate [24,25] .

Temperature [°C]	130
Pressure [bar]	22
Molar flowrate [kmol/h]	8612
Mass flowrate [ton/h]	216.2
CO fraction (%)	59.0
CO_2 fraction (%)	2.5
H_2 fraction (%)	20.8
H_2O fraction (%)	2.3
N_2 fraction (%)	15.1

In order to assess the technical and economic relapses of CO_2 capture and H_2 co-production, it was necessary to include in the simulation flowsheet the combined cycle section as well. A schematic of the block flow diagram of this further section considered in this study is reported in Figure 1.

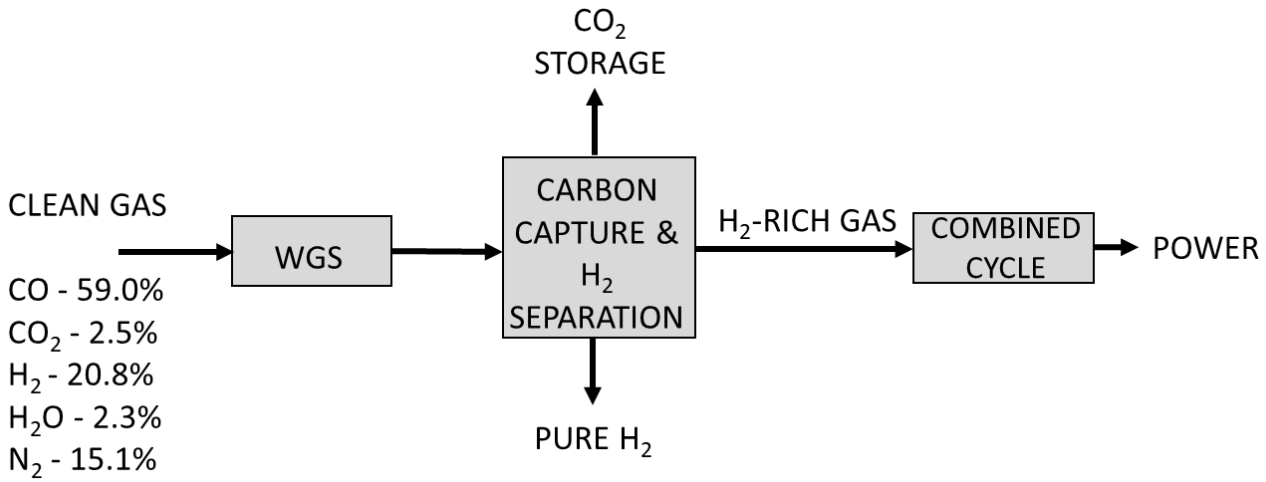

Figure 1: Block Flow Diagram of Water Gas Shift, carbon capture and hydrogen separation, combined cycle sections.

2.2 Water Gas Shift (WGS)

The pre-combustion capture of carbon dioxide and the production of high purity H_2 require the conversion of carbon monoxide and steam into CO_2 and H_2, coming with the clean syngas stream, by means of the Water Gas Shift (WGS) reaction. Namely:

$$CO + H_2O \leftrightarrow H_2 + CO_2 \quad (1)$$

The additional steps required by the WGS reaction implies a reduction of overall efficiency of the IGCC process [26] mainly due to lower calorific value of a hydrogen mole than the calorific value of a CO mole. The WGS reaction is carried out in two steps. The first one is the High Temperature Shift and is carried out at about 400 °C by means of a Fe_2O_4/Cr_2O_3 catalyst. The second one is the Low Temperature Shift and is carried out at about 200 °C by means of a Cu-ZnO-Al_2O_3 catalyst. This sequence allows to take advantage of the faster conversion rate in the HTS path and to finally approach a higher equilibrium conversion value (larger than 99%) for the most favourable equilibrium conditions in the LTS [27]. The main operating parameter of this process is the H_2O/CO molar ratio (Steam to Carbon, *SC*). In the simulation, this parameter was assumed equal to 2.5. The clean gas is heated from 130 °C to 400 °C and is mixed with a medium pressure superheated steam (22 bar, 400 °C). The adopted feed ratio was chosen to obtain a H_2O/CO molar ratio (Steam to Carbon, *SC*) equal to 2.5. The two fixed bed reactors, modelled as plug flow reactors, were sized to obtain a CO conversion of about 80% and 99%, respectively. To avoid sintering of the catalyst, the temperature in the HTS and LTS reactors was constrained to not exceed 600° C and 300° C, respectively. The maximum allowed pressure drop in the sequence of the two catalytic fixed bed, estimated by the Ergun equation, was assumed of about 2 bar. The kinetic expressions considered were taken by [28] for the HTS and [29] for LTS:

$$r = k_0 \exp\left(-\frac{E}{RT}\right) \frac{p_{CO}^m p_{H_2O}^n}{p_{CO_2}^o p_{H_2}^p} \quad (2)$$

the kinetics adopted for these two steps were taken from the literature and are reported in Table 2.

Table 2: Water Gas Shift catalysts properties.

	High Temperature Shift [28]	Low Temperature Shift [29]
Catalysts type	Fe_2O_4/Cr_2O_3	$Cu\text{-}ZnO\text{-}Al_2O_3$
Particle density [kg/m^3]	1250	1360
Diameter [m]	$4 \cdot 10^{-3}$	$4 \cdot 10^{-3}$
Sphericity factor	1	1
Bed void fraction	0.4	0.4
k_0 [kmol kg^{-1} s^{-1} kPa$^{(o+p-m-n)}$]	4.557	82.37
E [J/kmol]	$8.8 \cdot 10^7$	$5.93 \cdot 10^7$
M	0.9	1
N	0.31	1.9
O	0.156	1.4
P	0.05	0.9

The gas stream leaving the two WGS stages is cooled down to 30 °C to condense the steam.

2.3 CO_2 capture by Selexol®

For the case of the traditional process sketched in Figure 2, the section for CO_2 separation with the Selexol® technology is located after the WGS reactor and, thus, the inlet stream to the section is a clean syngas enriched in H_2 and CO_2 [30]. Differently, for the case of the innovative process sketched in Figure 3, the Selexol® section is located after the partial H_2 separation by membrane and, thus, the inlet stream is richer in CO_2.

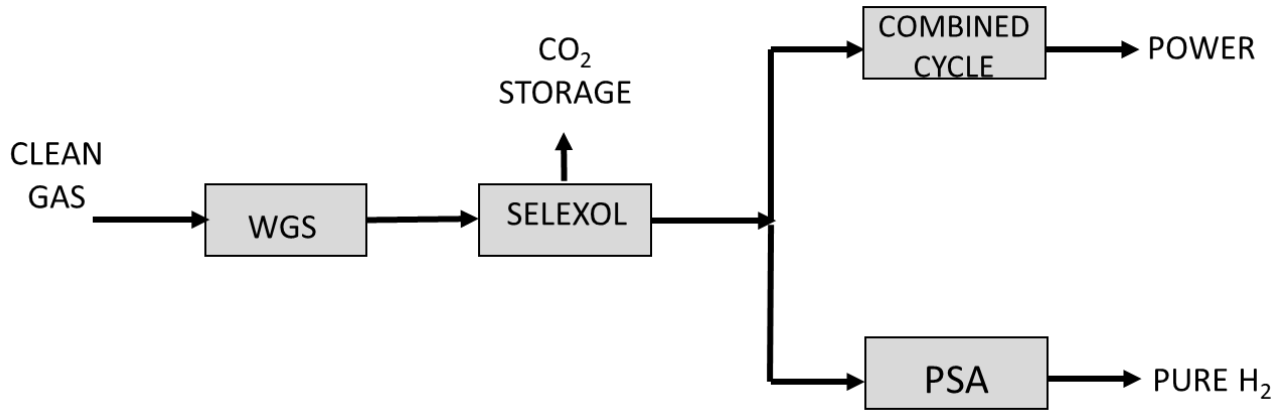

Figure 2: Process diagram of CO_2 capture and H_2 production section PSA to produce pure hydrogen.

Figure 4 shows the flowsheet of the section with the Selexol® technology. The separation of CO_2 from the enriched syngas stream is carried out by absorption in the proprietary solvent Selexol®, a

mixture of dimethyl ethers of polyethylene glycol ($CH_3O(C_2H_4O)_nCH_3$), where "n" is between 3 and 9, in a packed tower with 75mm IMTP® packing of Koch-Glitsch®.

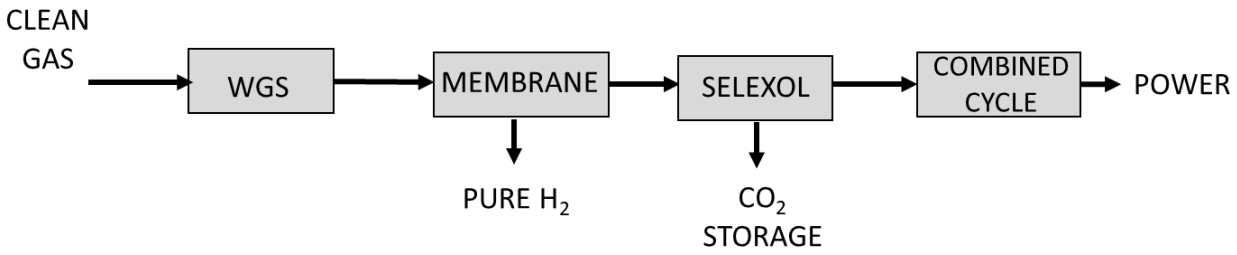

Figure 3: Process diagram of CO_2 capture and H_2 production section using membrane technologies to produce pure hydrogen.

The Selexol® solvent is sent to the top of the tower at 18 bar and 30 °C. Solvent regeneration is carried out downstream the absorption tower to separate carbon dioxide and to recycle the solvent. However, a small make-up stream is necessary to replace the solvent entrained in the gaseous stream leaving the packed tower. In particular, the regeneration is performed by lowering the pressure in two stages by means of two expansion valves (VALVE1 and VALVE2) up to 1 bar. In particular, the first valve expands the gas to an intermediate pressure, whose value has to be optimized depending on the required overall percentage of captured CO_2. An optional heat exchanger (HEATER) is placed between the two expansion stages to enhance the CO_2 recovery from the solvent stream. Three different values for the recovery of CO_2 were considered, namely 70%, 80% and 90%.

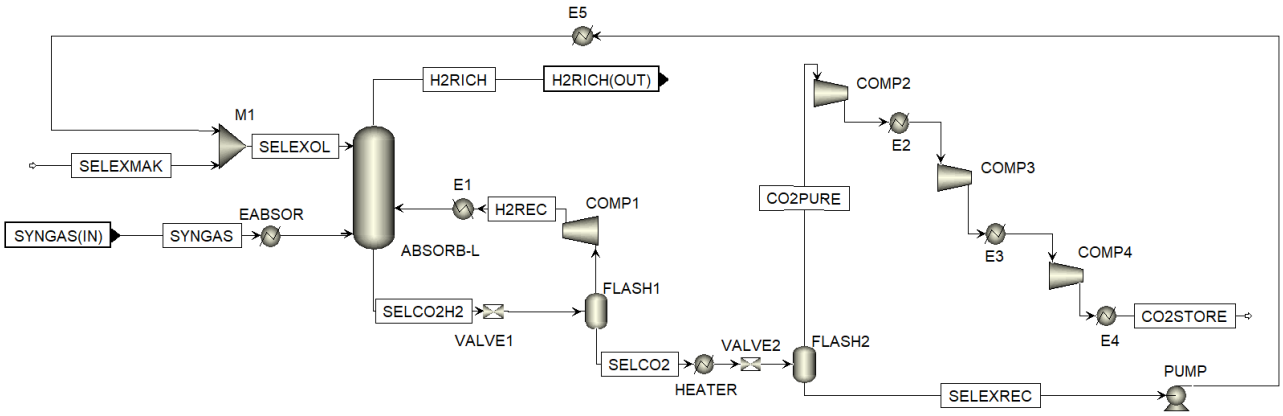

Figure 4: Process flowsheet of the CO_2 capture section.

The gas stream leaving the first flash (FLASH1), containing mostly H_2, CO_2 and N_2, is fed back to an intermediate section of the absorption tower in order to recover the hydrogen absorbed in the liquid stream. Hydrogen recovery, in fact, is a critical parameter to maximize the IGCC power and the pure

hydrogen production. The second flash is used to recover the CO_2 from the solvent. The regenerated solvent is mixed with the make-up stream and recycled back to the absorption tower after proper recompression. The recovered CO_2, which has the required purity (at least 98.5% by weight) is compressed up to 110 bar by a compressor train, formed by three compressors (COMP1, COMP2 and COMP3) with intercooling by two heat exchangers, for storage conditions.

The degrees of freedom for the design of this section include the pressure value after the first expansion stage and the temperature of the second flash unit. These values are expected to depend on the required overall fraction of captured CO_2

2.4 H_2 purification section by PSA

Figure 3 shows that the syngas, rich in H_2, leaving the section of CO_2 capture by Selexol® technology is splitted in two streams, the first to be sent to the combined cycle and the second to purification by Pressure Swing Adsorption (PSA), which ensures purities larger than 99.99%. The mass and energy balance on the overall IGCC process indicates that the value of the split ratio of hydrogen between the combined cycle and the PSA is lower limited. In fact, the smaller is the hydrogen flow rate to the combined cycle, the less is the high pressure steam produced in the Heat Recovery Steam Generator. As a result, the minimum hydrogen flow rate to the combined cycle is the value corresponding to the minimum amount of high pressure steam that is mainly required by the WGS reactor [26]. Accordingly, in the present case study the split ratio of hydrogen to combined cycle was assumed 80% and, thus, only 20% of the hydrogen was considered for the PSA section. The lower content of H_2 in the stream to the combined cycle is expected to produce a lower power output.

The PSA is a batch process consisting of a sequence of four steps: adsorption, depressurization, purge and pressurization. These steps are briefly described in the following.

2.4.1 Process simulation of PSA

The adsorption pressure and the purge ratio (P/F) are the operating variables of the PSA process. In our case, the operating pressure was fixed equal to the output pressure from the absorption column (18 bar). This in order to avoid compressing the syngas.

Adsorption

The inlet valve is opened and the syngas (rich in H_2, N_2 and CO_2) flows through the adsorbent bed. Pure H_2 is obtained at the outlet. The adsorption time is a fraction of the breakthrough time of N_2.

Depressurization

The inlet valve is closed. The pressure is decreased up to 1 bar. N_2 and CO_2 start desorbing thanks to the lower pressure and leaving the bed.

Purge

Since the pressure decrease is not sufficient for the complete regeneration of the adsorbent, part of the pure hydrogen, obtained during the adsorption step, is sent, in countercurrent, through the bed. This allows further desorption of previously adsorbed species, N_2 and CO_2, and, thus, the complete regeneration of the bed. The flowrate of pure H_2, *P*, sent to the bed during this step is related to the total feed rate of the adsorption step, *F*, by the so called product/feed ratio, *P*/*F*. On the one hand, the larger is the *P*/*F* ratio, the easier is the adsorbent regeneration. On the other hand, large *P*/*F* ratio values do not allow acceptable overall hydrogen recovery in the process.

Pressurization

The adsorbent bed is reported to the operating pressure of 18 bar. This step is carried out by opening the inlet valve, closing the outlet valve and feeding the syngas stream to be purified. Considering the intrinsic transient and the semi continuous characteristics of the process, multiple adsorbent beds are necessary to work simultaneously in order to obtain a continuous process. As a result, at least four beds are necessary to cover the four cyclic steps. Each cycle step has a characteristic time. Inherent constraints arise from related process operations. In particular, the adsorption step and the purge step need the same time because the bed operating in purge mode receives part of the H_2 coming from the bed operating in adsorption mode.

2.4.2 Adsorption model

Simulation of the four PSA steps and sizing of the adsorbent beds were performed by Aspen Adsorption® (version 8.0) simulation tool of Aspen One® suite. A one-dimensional mass balance model for the gas in the adsorbent fixed bed used by the simulator assumes plug flow with axial dispersion:

$$\frac{dy_i}{dt} + \frac{RT}{p}\rho\left(\frac{1-\varepsilon}{\varepsilon}\right)\frac{\partial q_i}{\partial t} + \frac{\partial(uy_i)}{\partial z} - D_{ax}\frac{\partial^2 y_i}{\partial z^2} = 0 \qquad (3)$$

For simplicity, isothermal conditions were also assumed. Pressure drop are calculated according to the Ergun equation.

Table 3: Adsorbent bed properties [31].

Adsorbent	Activated carbon (2GA-H2)
Shape	Cylindrical
Particle size	1.7 – 2.36 mm
Bed density (ρ)	0.525 g/cm^3
Superficial area	1025.17 m^2/g
Thermal capacity	1046.03 J/kg K
Void fraction (ε)	0.426

The adsorption rate of the adsorbent material was described according to equation reported by You et al. (2012):

$$\frac{dq_i}{dt} = \omega(q_i^* - q_i) \quad (4)$$

where q_i is the specific amount of species *i* adsorbed, ω is the mass transfer constant and q_i^* is the equilibrium assorbedc amount. The latter was evaluated according to the adsorption isotherm valid for multicomponent systems [31]:

$$q_i^* = \frac{q_{mi} B_i P_i}{1+\sum_{j=1}^{n} B_j P_j} \quad (5)$$

$$q_{mi} = k_{1,i} + k_{2,i} T \quad (6)$$

$$B_i = k_{3,i} \exp\left(\frac{k_{4,i}}{T}\right) \quad (7)$$

where q_i^* is the adsorbed amount of the component *i* at equilibrium, q_{mi} is the Langmuire-Freundlich isotherm parameter of the component *i*, P_i is the partial pressure of the component *i*.

Danckwerts boundary conditions were assumed for the ODE equation (4).

The special activated carbon (2GA-H2) is used to selectively adsorb N_2 and CO_2. Its adsorption properties appearing in equations (3 - 7) were taken from the literature [31] and are reported in Table 4.

Table 4: Adsorption isotherms parameters and transport constant for activated carbon (2GA-H2) [31].

	H_2	N_2	CO_2
k_1 [mol/kg]	9.35	4.11	25.89
k_2 [mol/kg K]	$-1.40 \cdot 10^{-2}$	$-1.06 \cdot 10^{-2}$	$-7.18 \cdot 10^{-2}$
k_3 [1/atm]	$7.55 \cdot 10^{-5}$	$4.70 \cdot 10^{-4}$	$9.34 \cdot 10^{-3}$
k_4 [K]	1081.43	1683	1012.76
ω [1/s]	0.2	0.48	0.039

Aspen Adsorption® considers the complete systems of valves and tanks necessary for the continuous operations. Results of the simulation provide with the time series of the molar fraction of H_2, N_2 and CO_2 at the exit of the adsorption beds. For the adsorption step these correspond to the breakthrough curves. Assuming a P/F ratio equal to 0.12, corresponding to a hydrogen recovery of 85%, the mass of adsorbent of four beds was sized in order to obtain a hydrogen purity larger than 99.99%. A life time of four years was assumed for the adsorbent.

The overall results of these simulations are reported in the steady state simulation flowsheet of Aspen Plus by means of an ideal separator with assigned purity and recovery for the hydrogen outlet stream.

2.5 H_2 purification by membrane process

Figure 4 reports the block flow diagram for the process with hydrogen separation by membrane and subsequent CO_2 separation by the Selexol® process. The partial separation of H_2 before CO_2 separation make the partial pressure of carbon dioxide increase at outlet of the membrane unit. This facilitates the Selexol® process for the CO_2 capture. The hydrogen obtained, after separation from the sweep gas, can be stocked directly. Using N_2 as sweep gas, to obtain pure H_2 a PSA section is necessary [32].

2.5.1 Sizing of membrane and process parameters

Palladium membranes were considered for the selective permeation of hydrogen [32]. In fact, permeation of other gas species can be neglected through these membranes. Units consisting of a bundle of tubular membranes in a shell were considered assuming that the syngas flow was inside the tubes. Superheated low pressure steam (1 bar and 350°C) was assumed as sweep gas flowing in countercurrent outside the membrane tubes in order to keep the partial pressure of hydrogen in the permeate as low as possible and to obtain a significant driving force for permeation. The choice of steam instead of nitrogen allows an easier separation from hydrogen by simple water condensation [27].

Assuming steady state conditions, one dimensional conservation equations can be written on hydrogen in the retentate and in the permeate streams [27]. Hydrogen diffusion in the membrane was described in the simulation by Fick-Sieverts' law. A set of ordinary differential equations of the first order was obtained. In these equations the dependent variables correspond to the flowrate of hydrogen in the retentate and in the permeate:

$$\frac{dF_{H_2,ret}}{dz} = -\frac{B_H}{\delta}\left(P^n_{H_2,ret} - P^n_{H_2,per}\right)\frac{A_{memb}}{L} \quad (8)$$

$$\frac{dF_{H_2,per}}{dz} = -\frac{B_H}{\delta}\left(P^n_{H_2,ret} - P^n_{H_2,per}\right)\frac{A_{memb}}{L} \quad (9)$$

with the following boundary conditions:

$$\text{z=0} \quad F_{H_2,ret} = F_{H_2,tot} \quad (10)$$

$$\text{z = L} \quad F_{H_2,per} = 0 \quad (11)$$

where $F_{H_2,ret}$ and $F_{H_2,per}$ are the H_2 flowrate in the retentate and in the permeate, B_H is the hydrogen permeability, δ is the membrane thickness, L is the membrane length, $P_{H_2,ret}$ and $P_{H_2,per}$ are the partial pressures of H_2 in the retentate and in the permeate, A_{memb} is the lateral area of the N tubular

membranes. The flow rate of other gas species on the retentate side and of steam on the permeate side are assumed constant assuming negligible permeation. Pressure drop were also neglected on both sides

The palladium membrane parameters were taken in the literature and are reported in Table 5 [32].

Table 5: Parameters of the palladium membrane [32].

Lifetime of membranes (year)	1
Temperature[°C]	350
Hydrogen permeability [kmol/m h bar^n]	$7.99\ 10^{-7}$
Membrane thickness [m]	$1\ 10^{-6}$
Retentate pressure [bar]	20
Permeate pressure [bar]	1
Membrane tube internal radius [m]	0.045
Membrane tube lenght [m]	5
n	0.96
Inert/purge ratio	0.1

Numerical solution of the ODEs was performed by means MATLAB® computing software using the *bvp4c* function for boundary value problems. Tube length was assumed equal to 5 m, while the number of tubes was sized in order to obtain the desired hydrogen recovery. The latter was varied between 10% and 20%

The numerical results of the membrane model were integrated in the steady state simulation flowsheet of Aspen Plus by means of an ideal separator with two outlet streams corresponding to the permeate and the retentate. Steam is then separated from hydrogen by condensation at 50°C. Hydrogen is compressed up to 18 bar in order to reach the same storage conditions of H_2 obtained by PSA.

2.6 Combined cycle and heat integration

The combined cycle consists of three sections:

- a gas turbine which burns the clean syngas gas (low CO_2) resulting from the capture sections;
- a Heat Recovery Steam Generator (HRSG) where the water and steam streams from the other sections of the IGCC arrive and further high pressure steam is generated using the flue gas from the gas turbine;
- three steam turbines using the high pressure, the medium pressure and the low pressure steam obtained in the HRSG unit [25];

Before entering the turbine, the clean syngas is saturated with water at medium pressure (22 bar), in order to avoid the formation of NO_x during combustion. The air flow rate sent to the turbine is calculated to obtain a flue gas temperature of 540 °C. The flue gases are used in HRSG to generate

other high-pressure steam (127 bar) which sums up to that generated for the thermal quench in the gasifier. The high-pressure turbine generates medium pressure steam (35 bar), which is combined with the medium pressure steam of the gasifier to expand into the medium pressure turbine. In turn, the produced low-pressure steam (6 bar) is expanded into the low pressure turbine.

A thermal integration of the CO_2 capture and removal section was optimized in order to maximize the production of electricity even when the capture is present.

In the process section dedicated to CO_2 capture, several heat exchange units are present in order to obtain gaseous streams at the required temperatures. This integration has been approached with the aid of the pinch theory, in order to possibly avoid, or else to minimize, the request for hot utilities, necessary for the various thermal transformations.

To construct a suitable heat exchange network of the water gas shift and CO_2 removal section, a minimum temperature difference between the hot and cold current of each exchanger equal to 20 °C was assumed in order to limit the exchange are and the related investment costs otherwise required by high-level exchangers allowing lower temperature differences between streams.

The hot utility used consists of a fraction of the flue gas exiting the gas turbine at 540 °C.

3 Technical Results

3.1 Process results

In the WGS section CO was transformed to CO_2 and H_2 using H_2O as reactant. By a sensitivity analysis, both reactors filled with the respective catalysts described in paragraph 2.2 have been dimensioned with the measures of 8 m in length and with a diameter of 6 m. The local conversions obtained were 79.5%, for HTS reactor, and 94.1%, for LTS reactor. In this way, it is accomplished an overall CO conversion of about 99%. A heat exchanger lowers the temperature down to the 210 °C operating temperature of the catalyst in the second reactor. The total pressure drop in two reactors was of about 1.73 bar. So, a gas rich in H_2, CO, CO_2 and H_2O was obtained at a pressure of 20.27 bar. Finally, the water could be easily separated from the syngas by condensation.

Table 6: Composition and conditions of CO_2 and H_2 rich syngas.

Temperature [°C]	30
Pressure [bar]	20
Molar flowrate [kmol/h]	12098
Mass flowrate [ton/h]	309
CO fraction (%)	0.5
CO_2 fraction (%)	38.9
H_2 fraction (%)	50.7
H_2O fraction (%)	0.2
N_2 fraction (%)	9.7

Table 7 shows the most critical condition for CO_2 capture are for a recovery of CO_2 about 90%. To capture more carbon dioxide from the syngas, a higher amount of solvent in the adsorption unit (DEPG/syngas ratio) and a higher volume of the absorption column itself are required. The DEPG/syngas ratio increases with the capture fraction. Namely, the ratio increases of about 25% passing from a value of 2.4 for 70% of cabon capture to a value of 3.0 for 90% of carbon capture Moreover, to reach 90% of CO_2 recovery, a thermal regeneration of the solvent was necessary. The liquid stream leaving the first flash was heated up to 50 °C. Increasing the temperature a higher volatilization of CO_2 was achieved in order to reach the recovery target.

The very high vaporization temperature of Selexol® (more than 200 °C) allows to maintain the liquid state either during the absorption phase and in that of regeneration. A very high power for the CO_2 compressor train was required (more than 20 MW), increasing up to 26 MW for the highest flowrate of CO_2 stream (90% of recovery). In Table 7, all process parameters selected for the cases of 70%, 80% and 90% of CO_2 removal are shown.

Table 7: Optimal process values for the carbon capture section for the process flowsheet of Figure 2.

CO_2 capture (%)	**70**	**80**	**90**
DEPG/Syngas (mol/mol)	2.4	2.6	3.0
Column diameter (m)	6	6	6
Column height (m)	20	35	40
Pressure of FLASH1 (bar)	7	7	9
Regeneration temperature (°C)	30	30	50
Make-up Selexol® (kmol/h)	0.005	0.006	0.063
Low Pressure Steam (MW_t)	0	0	120
Pump power (MW_e)	4.7	5.1	6.0
Compressor power (MW_e)	0.6	0.8	0.2
Compressor train power (MW_e)	20.0	22.7	26.7
Purity of CO_2 stream (%)	99.66	99.74	99.06

For the case with hydrogen production by PSA, the adsorbent bed volume increases with the H_2 recovery. The optimal values for the beds volume, minimizing investment costs, are the same for the three values of CO_2 recovery, 70%, 80% and 90%. This is due to the assigned separation efficiency of N_2 that is the limiting species in the adsorption step. In fact, in order to keep a H_2 purity higher than 99.99%, the lower P/F ratio necessary to combine the highest H_2 recovery is equal to 0.12 using a bed volume equal to 26.92 m^3.

The palladium membranes used to recovery pure hydrogen were sized as described in the section 5.2. The length of membrane tubes was fixed to 5 m and the radius to 0.045 m (Table 5), while the numbers of tubes needed to permeate hydrogen change according to the desired hydrogen recovery (in the base case 20%). As result, a pure hydrogen amount in the permeate is obtained equal to 1362 kmol/h with a total number of tubes equal to 235 corresponding to an area about 332 m^2.

Table 8: Optimal process values of carbon capture section for the process flowsheet of Figure 3 with a pure hydrogen recovery equal to 20%.

CO_2 capture (%)	70	80	90
DEPG/Syngas (mol/mol)	2.0	2.4	2.8
Column diameter (m)	6	6	6
Column height (m)	30	35	35
Pressure of FLASH1 (bar)	13	13	13
Regeneration temperature (°C)	30	30	50
Make-up Selexol® (kmol/h)	0.005	0.005	0.060
Low Pressure Steam (MW_t)	0	0	98
Pump power (MW_e)	3.5	4.2	5.0
Compressor power (MW_e)	0.03	0.03	0.04
Compressor train power (MW_e)	20.0	23.1	26.9
Purity of CO_2 stream (%)	98.82	98.71	98.52

As shown in Table 8, the amount of solvent necessary to remove the CO_2 from the gaseous stream is lower than the amount needed in the base case, without the hydrogen recovery by membranes carried out previously (Table 7). Even in this case the solvent/syngas ratio increases with the capture percentage increasing of about 40% passing from a value of 2.0 for 70% of carbon capture to a value of 2.8 for 90% of carbon capture.

The optimal size of the Selexol® absorption column is comparable with the case without the use of membranes. In the case of high capture efficiency (80-90%) the height required is higher and it is equal to 35 m. The flash pressure for the hydrogen recovery from the bottom stream of the column is higher (13 bar) thanks to the lower amount of hydrogen in the solvent stream. Consequently a lower power is obtained (0.03-0.04 MW instead of 0.6-0.8 MW) in order to bring back the gas recycle stream at 20 bar. The thermal regeneration is necessary only in the case of 90% by using a lower vapor amount (98 MWt). Compared to the case without the membrane there are no differences in terms of CO_2 purity.

3.2 Power and efficiencies results

Simulation results in terms of material and energy balances were used to derive the technical performance of the whole IGCC plant. The main outputs are the electric power produced by the combined cycle and the possibly co-produced hydrogen. In particular, the net electric power was calculated by subtracting the auxiliary power absorbed by the plant to the gross electric power. Auxiliary power is mainly made of the electricity required by the Air Separation Unit (ASU), the

compressor train for CO_2 storage and the solvent recycle pump for the Selexol® process. In order to obtain an energy output for the hydrogen co-production consistent with the electric power, it is convenient to calculate the equivalent power of the hydrogen stream flow rate, $\dot{m}_{H2}$, by means of its low heating value, LHV_{H2}:

$$Power_{H_2} = \dot{m}_{H2} LHV_{H2} \quad (12)$$

The energy performance of the plant was assessed by estimating the net efficiency as follows [33]:

$$\eta_{net} = \frac{Power_{net} + Power_{H_2}}{\dot{m}_{feedstock} LHV_{feedstock}} \quad (13)$$

where $Power_{net}$ is the net electric power, $\dot{m}_{feedstock}$ is the feedstock flow rate, $LHV_{feedstock}$ is the low heating value of the feedstock. It can be argued that this efficiency formula is based on the sum of two inconsistent terms, the net electric power and the power generated by hydrogen oxidation. However, it is commonly used as a reasonable indicator considering the high efficiency of hydrogen conversion by means of fuel cells with cogeneration [34].

A common environmental impact indicator for power plant is the specific emitted CO_2 calculated as the ratio between the mass flow rate of emitted CO_2 and the net electric energy.

IGCC with CO_2 capture

In Table 9 are summarized the main technical results of the IGCC plant for all studied cases. For the sake of comparison, Table 9 also reports the base case without CO_2 capture and without hydrogen co-production, that correspond to the reference case of the IGCC plant of Puertollano [24]. As expected and commonly reported in the literature, the CO_2 capture before combustion reduces the gross power produced by the IGCC plant that produces only electricity due to the lower gas flow rate sent to the gas turbine. In particular, the gross power decreases from 315 MW to 266 MW by increasing the CO_2 capture from 0% to 90%. In addition to this, it can be noted that also the auxiliary power increases with carbon capture percentage. In fact, the auxiliary power without CO_2 capture is 35 MW [35]. In the case of carbon capture additional auxiliary power of the same order of magnitude is required for CO_2 compression (20, 23 and 27 MW for 70%, 80% and 90% CO2 capture, respectively). The further request of auxiliary power due to Selexol® recycle pump resulted to be much lower than that required for CO_2 compression (4.7, 5.1, 6.0 MW for 70%, 80%, 90% of CO_2 capture, respectively).

The overall reduction of net power determines an energy penalty of at least ten points, that is a decrease of the net efficiency of at least ten points for all the cases with CO_2 capture. These values are in agreement with those reported in literature for similar cases [36]. Finally, further inspection of Table 9 reveals that the specific emitted CO_2 decreases with increasing percentage of CO_2 capture. However, the fractional reduction of the specific emitted CO_2 is slightly lower than the CO_2 fractional

capture value. In fact, as reported above, the CO_2 emission decrease involves a net power decrease as well.

IGCC with CO_2 capture and hydrogen co-production

Table 9 shows that hydrogen co-production makes the net electric power decrease in favor of an increase of the equivalent power of hydrogen with both investigated technologies. As a result, for the case of 20% of hydrogen sent to purification, the net efficiency calculated according to Equation (13) reaches about 34%, that is four points higher than the obtained in the cases with CO_2 capture only. On the other hand, an apparent increase of about 20% of the specific CO_2 emissions is observed. This is due to the lower net electric power, which appears at the denominator of the specific CO_2 emission by definition.

Further analysis of Table 9 highlights some energy advantages of membrane technology with respect to the conventional PSA technology. First of all, differently for membranes, the separation recovery of PSA can not be complete due to the loss of hydrogen in the purge stream. This makes the H_2 equivalent power produced by PSA lower than that produced by membranes. Furthermore, positioning the CO_2 capture Selexol process after the H_2 separation by membranes makes the necessary solvent flow rate lower than in the process scheme with PSA where the Selexol process treats the larger stream leaving the WGS reactors. This makes the auxiliary power consumed for the solvent recompression lower for the flowsheet with membranes. On the whole, the sum of net electric power and of H_2 equivalent power is higher for the membrane cases. Therefore, the net efficiency is at least one point higher.

The specific emitted CO_2 (ton_{CO2}/MWh) in the base case is equal to 0.83 ton_{CO2}/MWh and it decreases when the percentage of carbon capture increases. the lowest value is obtained with carbon capture 90% for all cases considered: simple capture, hydrogen production by PSA, hydrogen production by membranes. Therefore, the quantity of captured CO_2 compensates the reduction of net power production due to the section of capture (Table 9). The minimum value of specific emitted CO_2 is obtained for only carbon capture 90% (0.1 ton_{CO2}/MWh) while for PSA/membrane with carbon capture 90% a value of 0.13 ton_{CO2}/MWh is obtained. This because when also pure hydrogen is produced the net electricity produced decreases.

435 *Table 9: Main results for the IGCC plant*

	Base Case	CO_2 Capture only			20% H_2 production by PSA			20% H_2 production by membrane		
% CO_2 Capture	0	70	80	90	70	80	90	70	80	90
Gross power (MW)	315.0	269.4	268.9	266.0	220.9	220.7	219.6	221.0	220.7	219.7
Base case auxiliary power (MW)	35.0	35.0	35.0	35.0	35.0	35.0	35.0	35.0	35.0	35.0
Compression train power (MW)	0.0	20.1	22.8	26.7	20.1	22.8	26.7	20.1	22.8	26.7
Selexol® pump power (MW)	0.0	4.7	5.1	6.0	4.7	5.1	6.0	3.5	4.2	5.0
H_2 compressor power (MW)	0.0	0.0	0.0	0.0	0.0	0.0	0.0	6.0	6.0	6.0
Total auxiliary power (MW)	35.0	59.8	62.9	67.7	59.8	62.9	67.7	64.6	68.0	72.7
Net power (MW)	280.0	209.9	206.1	198.3	161.4	157.8	151.9	156.7	152.7	146.8
Specific emitted CO_2 [ton_{CO2}/MWh]	0.83	0.31	0.20	0.10	0.40	0.26	0.13	0.41	0.27	0.13
H_2 equivalent power (MW)	0.0	0.0	0.0	0.0	75.2	76.5	76.6	90.8	90.8	91.1
Total investment cost (M€)	419	492.8	497.9	501.5	530.45	535.8	541.08	566.5	570.5	576.5
Specific Investement [M€/MWe]	1.50	2.35	2.42	2.53	3.25	3.35	3.51	3.61	3.77	4.01

436

4. Economic Results

4.1 Economic results for IGCC with CO_2 capture

For the economic analysis, a total investment cost of the IGCC plant without carbon capture was assumed about 419 M€ [37]. The investment cost of the additional process sections for Water Gas Shift, CO_2 capture and H_2 separation were estimated on the basis of the simulation results. In particular, the capital cost of the process unit was calculated by typical power law of unit capacity or size. Total capital investment estimates were derived by multiplying the equipment cost by Lang factors.

The capital investment of each section is reported in Figure 5. To separate CO_2 other 31 M€ are necessary to have the WGS section.

Selexol® impacts on capital costs for 28, 32, 34 M€ to capture 70%, 80%, 90% of CO_2 respectivelly. While 15, 16, 17 M€ are necessary for the compressor train of CO_2 for 70%, 80%, 90% of CO_2 respectively.

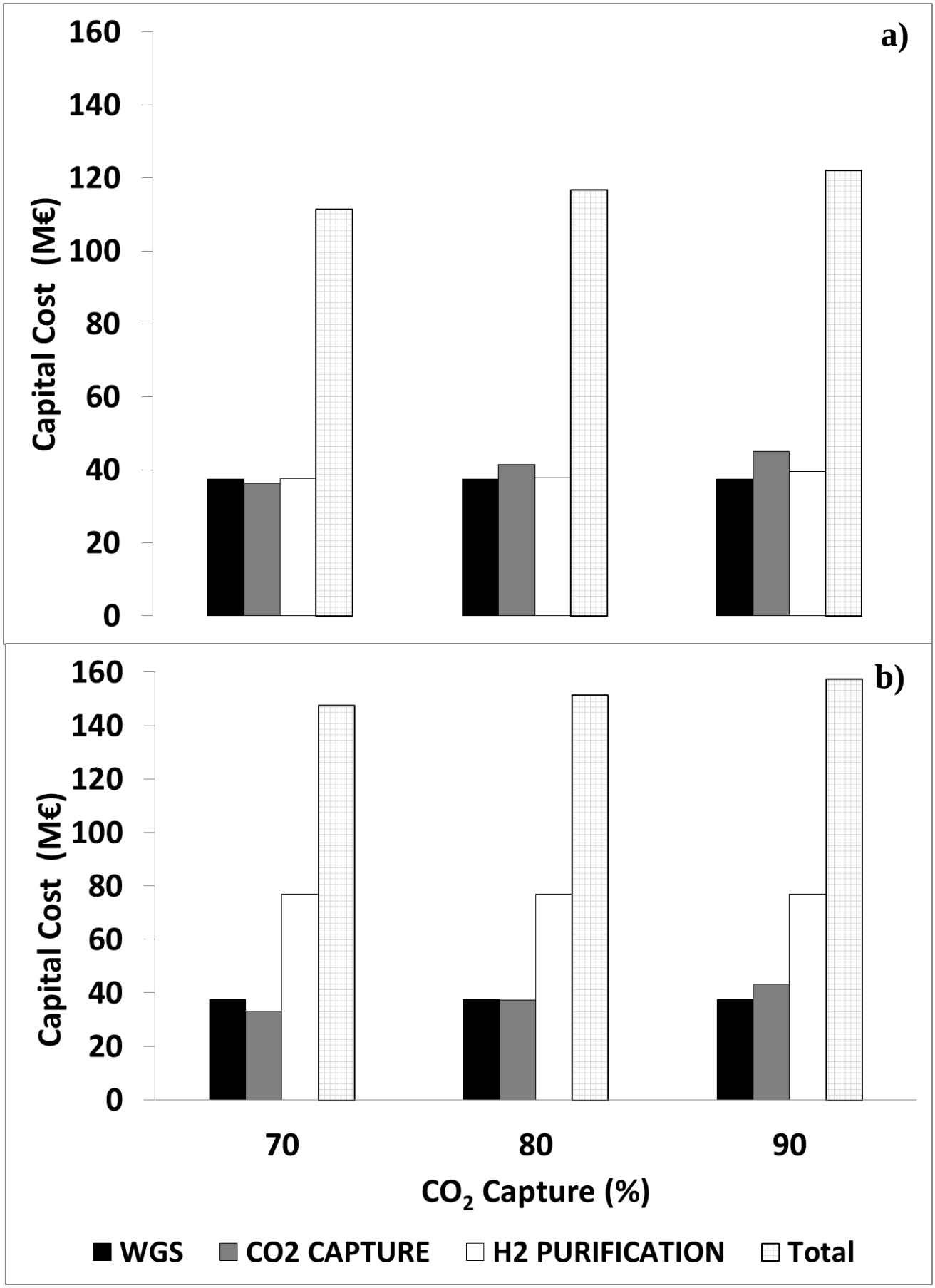

Figure 5: Capital cost distribution for: a) hydrogen production by PSA and b) hydrogen production by membrane.

The total annual cost of the process was estimated as the sum of operational cost and feedstock purchasing cost. The operational cost (*OPC*) includes the maintenance and labour cost (*MLC*), process utility (steam) cost (*STMC*), natural gas cost (*NGC*), and power cost (*PWC*) [38]:

$$OPC = MLC + STMC + NGC + PWC \quad (14)$$

The investment costs are the sum of IGCC costs without CO_2 capture and costs of CO_2 capture section. The total investment costs of IGCC with CO_2 capture are shown in Table 9.

For the case of CO_2 removal by the Selexol®, the investment costs increase between 18% and 20% respect the base case without CO_2 capture. The most significant cost is the compression of carbon dioxide, which is essential for its liquefaction and storage.

Subsequently, the discounted cash flow analysis allowed to calculate the cost of electricity (COE). COE consists in the minimum selling price of electricity so that it returns the initial investment in the life-time of the plant. The life-time in this case was assumed of 25 years [24].

Table 10: Main assumptions for the economic analysis

Economic parameter	Value
Life time of the IGCC (y)	25
Plant construction time (y)	4
Working capital (% of Total Investment Cost)	2
Manufacturing costs (% of Total Investment Cost)	1.1
Insurance (% of Total Investment Cost)	2
Discount rate (%)	7.5

In agreement with the previous works, the cost of mitigation of CO_2 capture was also calculated. This is the cost to sustain per ton of CO_2 avoided in atmosphere. This concept has been developed to assess potential greenhouse gas reduction. The mitigation cost is defined as:

$$CO_2 avoided\ cost = \frac{COE|_{CO2capt} - COE|_{casobase}}{CO_{2emitted}|_{basecase} - CO_{2emitted}|_{CO2capt}} \quad (15)$$

The numerator represents the difference between COE with capture and COE of case base without capture. The denominator is the difference between the amount of CO_2 emitted with CO_2 capture and the CO_2 emitted without capture. The cost of mitigation is useful for comparing different capture technologies and finding if the mitigation cost is comparable with the carbon tax value.

In Figure 6, the cost of electricity production COE has an increase of 38% passing from the case with 70% of capture and to the case of 90% of capture. As regards mitigation costs, in all three cases the

mitigation cost is higher than 30 €/ton_{CO2}, which greatly exceed the average values of the carbon tax (20 €/ton_{CO2}). For 80% of CO_2 capture the mitigation cost is equal to 34 €/ton_{CO2}. This value is lower than mitigation cost for 90% case and it is lower than mitigation cost also for 70% of capture. This result is from a low increasing of COE for 80% case (about 2.9%) corresponding to a decrease of CO_2 emitted of about 10%. Overall, the capture of CO_2 by Selexol® technology is an economically not sustainable operation.

The lowest value of mitigation costs was obtained for 80% of CO_2 captured. In such conditions a compromise is reached between the investment costs necessary for the implementation of CCS section and the amount of captured CO_2.

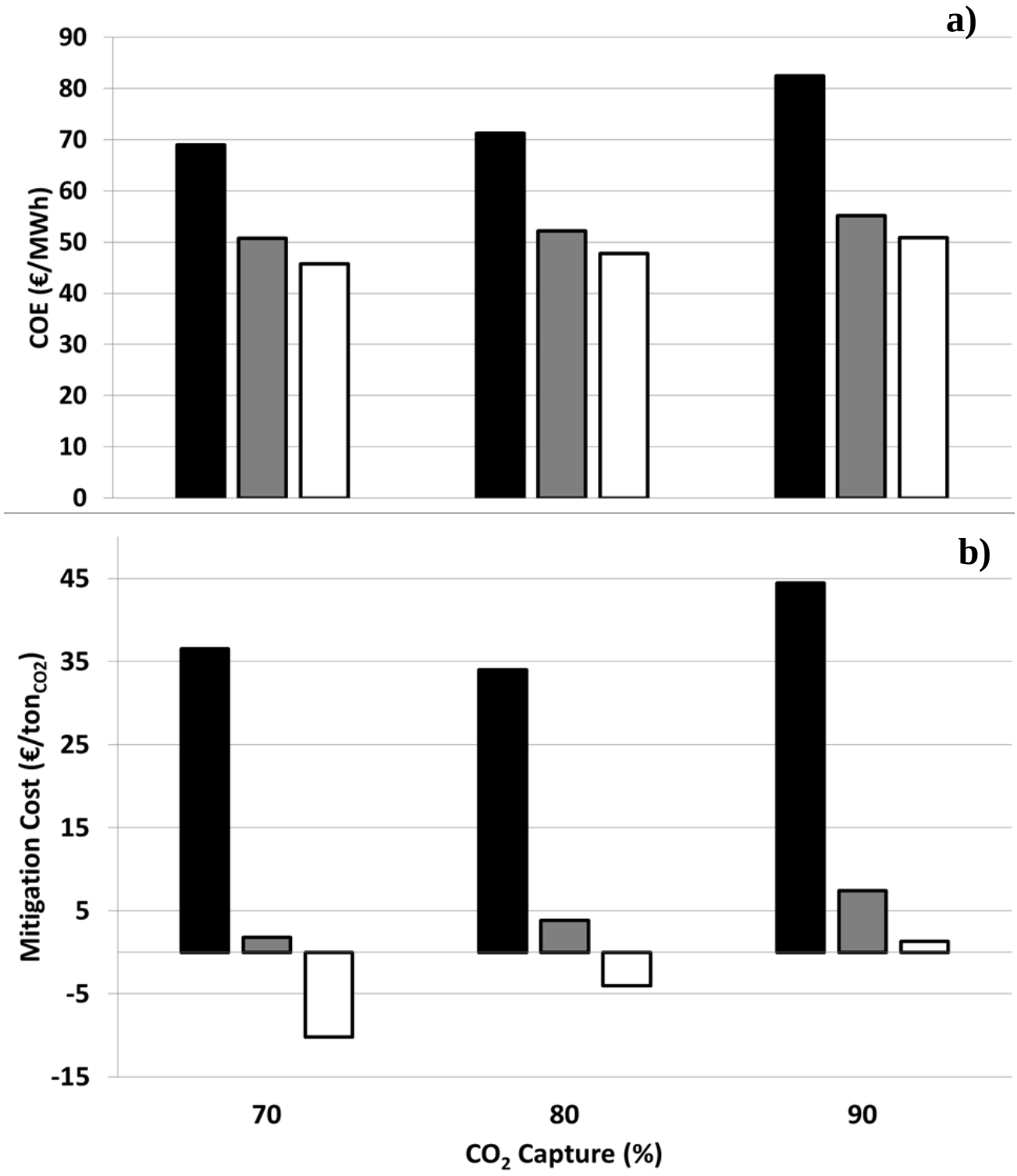

Figure 6: Main economic indexes, a) COE and b) Mitigation cost, for the CO_2 capture alone (black), the CO_2 capture with 20% H_2 production by PSA (grey),), the CO_2 capture with 20% H_2 production by membrane (white).

4.2 Economic results for IGCC with CO_2 capture and co-production of pure H_2

At present, CO_2 capture is not practiced because of too high costs to be incurred. In particular, as above demonstrated, the CO_2 mitigation costs appear to be higher than carbon tax. The high value-added high-purity hydrogen can represent a considerable source of income and, together with the removal of CO_2 capture, it can be a viable way. The sale price of hydrogen considered is 3 €/kg, in which the costs of compression, storage and delivery to customers are not considered.

The economic indices of an IGCC plant with and without production of hydrogen by PSA process are shown in Figure 6.

For unchanged CO_2 capture efficiency, the case with co-production of pure hydrogen shows a significant decay of the COE and the mitigation cost. The sale of hydrogen, contextually to power production, can be considered as an added value for the capture and storage of carbon dioxide. In addition, the values of the mitigation cost with the use of the PSA process have values comparable to the carbon tax in several European countries (30 €/ton_{CO2}). This also because the operating costs of PSA are considered absent.

For the case of palladium membranes, despite the high investment cost of membranes, the pure H_2 sale allows to considerably lower the mitigation cost for the capture of CO_2, which reaches its minimum for a 70% of CO_2 captured (10.11 €/ton_{CO2}). In this case, the mitigation cost is proportional to the post membrane capture percentage, by Selexol®. With this configuration the membranes represent a valid alternative to the traditional PSA process to make high purity H_2.

4.3 Comparison of economic indices between PSA and palladium membranes

Capturing and storing the carbon dioxide involves a cost per unit mass of CO_2 higher than the average carbon tax at European level (20 €/ton_{CO2}) in force today [39]. Selling pure hydrogen (20%) on the market, instead of expanding it in the turbines, can represent a sustainable alternative from a technical and economic point of view. Considering the same specific emitted CO_2 (70%, 80%, 90% of CCS) the mitigation cost of a ton of CO_2 captured in a plant with palladium membranes to produce hydrogen is always higher than mitigation cost obtained by traditional PSA process. This thanks to the COE higher for membrane cases (from 46 to 51 €/MWhe). Considering constant the carbon capture, the Selexol + PSA energy plants produce more energy than the membrane + Selexol plants, but less pure hydrogen, that in this analysis is prevailing on electricity selling, considering an Hydrogen selling price of 3 €/kg.

4.4 Sensitivity analysis on hydrogen recovery by membranes

A sensitivity analysis was performed varying the H_2 recovery of the highly selective membranes. The 20% recovery value used in the base case was varied to 10 and 15% in order to find the critical value of hydrogen to be produced to ensure the economic sustainability of the process with CO_2 capture.

The generated electric power decreases with increasing amount of pure hydrogen produced, which results in fact in a decrease of fuel gas to the combined cycle. On the other hand, the net efficiency according to equation (13) increases with increasing H_2.

Results in terms of the economic indexes cost of electricity COE and mitigation cost MC are reported in Figure 7. As expected, the COE decreases with increasing production of hydrogen. In particular, for 15% and 20% hydrogen recovery the COE approaches values of about 50 €/MWh which is comparable with the value without carbon capture reported by Sofia et al. [24]. This result can be explained by considering that the increasing productivity of high added value hydrogen is able to compensate the additional capital cost due to the separation and purification sections. Moreover, increasing the CO_2 capture from 70% to 90% determines an increase of the COE of about 15%. The trend of the mitigation cost is consistent with that of the COE. In fact, the mitigation cost decreases significantly with increasing hydrogen recovery. In particular, the mitigation cost becomes negative for a 20% hydrogen recovery. This means that the resulting COE with CO_2 capture is even lower than the COE without CO_2 capture thanks to the hydrogen revenues. Comparing the results for 15% and for 20% hydrogen recovery it can be concluded that the critical value of the hydrogen recovery that makes the mitigation cost equal to zero can be found in this range.

4.5 Sensitivity analysis on the cost of palladium membranes

Inspection of Figure 5 reveals that the capital cost of palladium membranes for H_2 separation is the most significant contribution to the additional investment cost for the new process sections. On the one hand, a possible increase of the palladium demand for large scale applications could determine a market price increase [40]. On the other hand, the continuous advancement in the thin layer palladium membrane technology may cause a reduction of their fabrication cost [41]. As a result, in order to take into account the uncertainty of the future scenario, a sensitivity analysis of the effect of the cost of membrane per unit surface on the profitability was carried out. In particular, the cost values considered were varied by a +50% and -50% of the membrane base cost of 10800 $/m^2 derived from DOE [42]. The results of this analysis are also reported in Figure 7 in terms of cost of electricity COE and mitigation cost MC. Inspection of the plots indicate that a 50% variation of the membrane price determines a COE change of about 3%, 5% and 10% for a 10%, 15% and 20% H_2 recovery, respectively. Correspondingly, a moderate change of the mitigation cost by 3-6 EUR per CO_2 ton results for the three values of hydrogen recovery.

A comparison with the results reported in Figure 6 reveals that the maximum value of the membrane price, 13600 €/m^2, returns values of COE (55 €/MWhe), and of mitigation cost (5 €/ton$_{CO2}$) equal to those obtained for the PSA technology for the case of a 20% hydrogen recovery with 90% CO_2 capture. For the lower values of CO_2 capture, 70% and 80%, lower hydrogen recovery is sufficient to ensure the economic equivalence between the membrane technology and the PSA technology.

562

563

564

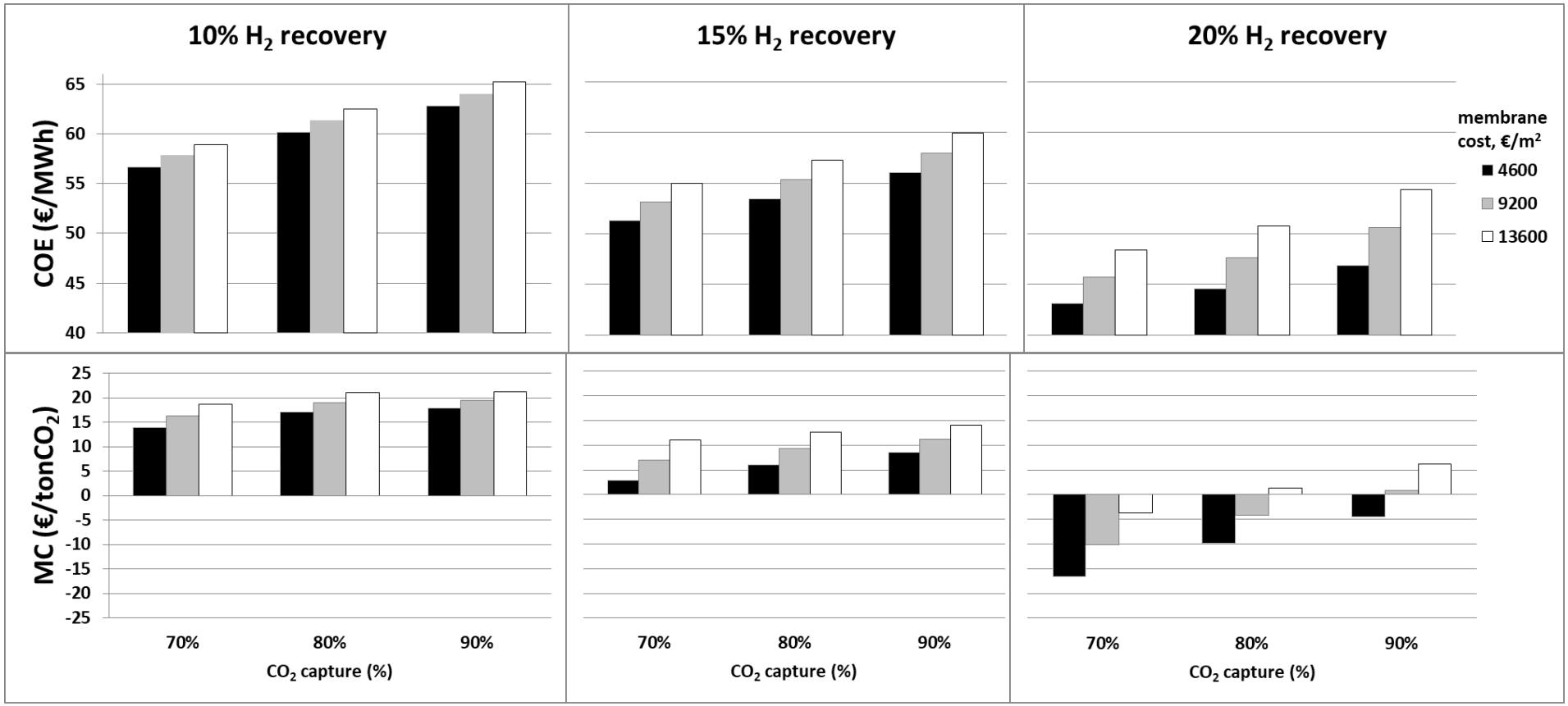

Figure 7 *Cost of electricity and mitigation costs as a function of carbon capture, hydrogen recovery and palladium membrane cost*.

5 Conclusions

The process simulations performed in this study confirmed that, in IGCC plants with coal feedstock, CO_2 capture between 70% and 90% causes up to 30% loss on net produced power which corresponds to about 10% energy penalty in terms of efficiency. This corresponds to a mitigation cost between 35 and 47 €/ton$_{CO2}$, which are consistently higher than the average current carbon tax.

Moreover, it was demonstrated that the indroduction of a new process section aiming at the coproduction of pure hydrogen, using either conventional PSA technology or innovative palladium membrane technology, significantly lowers the additional cost of electricity and, makes the mitigation cost of CO_2 capture much more sustainable.

In particular, assuming a hydrogen selling price of 3 €/kg and a palladium membrane cost of 9200 €/m^2 , the mitigation cost of 90% CO_2 capture drops below 5 €/ton$_{CO2}$ provided a 20% hydrogen recovery. This result was shown to be even more convenient than that achievable by conventional PSA technology.

A sensitivity analysis showed that reducing the hydrogen recovery to 10% and 15%, using the membrane technology, still allows COE values below 65 €/MWhe and, thus, mitigation cost values below 20 €/ton$_{CO2}$. Of course, even lower costs were obtained for 70% and 80% CO_2 capture.

Finally, a sensitivity analysis on the membrane cost per unit surface showed that even a 50% increase of the fabrication cost could determine a COE increase of only about 10% and a mitigation cost increase of only about 5 €/ton$_{CO2}$.

Symbols

A_{memb} = lateral membrane area (m^2)

B = Adsorption isotherms parameter (1/atm)

B_H = hydrogen permeability (kmol/m h bar^n)

D_{ax} = dispersion coefficient on direction z (m^2/s)

E = activation energy (J/kmol)

$F_{H_2,per}$ = Flowrate of hydrogen in the membrane permeate (kmol/h)

$F_{H_2,ret}$ = Flowrate of hydrogen in the membrane retentate (kmol/h)

$F_{H_2,tot}$ = Total flowrate of hydrogen in the membrane (kmol/h)

k_0 = reaction rate constant (kmol kg^{-1} s^{-1} kPa$^{(o+p-m-n)}$)

k_1 = Adsorption isotherms parameter (mol/kg)

k_2 = Adsorption isotherms parameter (mol/kg K)

k_3 = Adsorption isotherms parameter (1/atm)

k_4 = Adsorption isotherms parameter (K)

L = membrane length (m)

$\dot{m}_{feedstock}$ = Feedstock flowrate (kg/s)

$\dot{m}_{H2}$ = Hydrogen flowrate (kg/s)

n = partial pressure exponent (-)

N = number of membrane tubes (-)

o, p, m, n = exponents of partial pressure

P/F = product/feed ratio (-)

$P_{H_2,per}$ = partial pressures of H_2 in the retentate (bar)

$P_{H_2,ret}$ = partial pressures of H_2 in the retentate (bar)

$Power_{H_2}$ = Equivalent power of hydrogen

$Power_{net}$ = Net Power of the IGCC plant

p_i = partial pressure of component i (kPa)

q_i = specific amount of species i adsorbed (kmol/m^2)

q_i^* = equilibrium amount adsorbed of the component i (kmol/m^2)

q_{mi} = Langmuire-Freundlich isotherm parameter of the component i (kmol/m^2)

r = reaction rate (kmol kg^{-1} s^{-1} kPa$^{(o+p-m-n)}$)

R = ideal gas constant (J kmol^{-1} K^{-1})

t = time (s)

T = temperature (K)

u = axial velocity on direction z (m/s)

y_i = molar fraction (mol/mol)

z = axial dimension (m)

δ = membrane thickness (m)

ε = void fraction

η_{net} = Net efficiency of the IGCC plant

ρ = bed density (g/cm^3)

ω = mass transfer constant (1/s)

Abbreviations

$COE|_{casobase}$ = Cost Of Energy without carbon capture (€/MWhe)

$COE|_{CO2capt}$ = Cost Of Energy with carbon capture (€/MWhe)

$CO_{2emitted}|_{basecase}$ = CO_2 emitted without carbon capture (ton_{CO2}/MWhe)

$CO_{2emitted}|_{CO2capt}$ = CO_2 emitted with carbon capture (ton_{CO2}/MWhe)

IGCC = Integrated Gasification Combined Cycle

$LHV_{feedstock}$ = Low Heat Value of feedstock (MJ/kg)

LHV_{H2} = Low Heat Value of hydrogen (MJ/kg)

MC = Mitigation Cost (€/ton_{CO2})

MLC = maintenance and labour cost (€/y)

NGC = natural gas cost (€/y)

OPC = operational cost (€/y)

PSA = Pressure Swing Adsorption

PWC = power cost (€/y)

$STMC$ = process utility cost (€/y)

References

[1] Pachauri RK, Meyer L. Climate Change 2014 Synthesis Report. 2014.

[2] Boyce JK. Carbon Pricing: Effectiveness and Equity. Ecol Econ 2018;150:52–61. doi:10.1016/J.ECOLECON.2018.03.030.

[3] An overview of IGCC systems. Integr. Gasif. Comb. Cycle Technol., Woodhead Publishing; 2017, p. 1–80. doi:10.1016/B978-0-08-100167-7.00001-9.

[4] Carpenter SM, Long HA. Integration of carbon capture in IGCC systems. Integr. Gasif. Comb. Cycle Technol., Woodhead Publishing; 2017, p. 445–63. doi:10.1016/B978-0-08-100167-7.00036-6.

[5] Baufumé S, Hake JF, Linssen J, Markewitz P. Carbon capture and storage: A possible bridge to a future hydrogen infrastructure for Germany? Int J Hydrogen Energy 2011;36:8809–21. doi:10.1016/j.ijhydene.2011.04.174.

[6] Cormos CC. Evaluation of energy integration aspects for IGCC-based. Int J Hydrogen Energy 2010;35:7485–97.

[7] Ahmed U, Zahid U, Jeong YS, Lee CJ, Han C. IGCC process intensification for simultaneous power generation and CO2capture. Chem Eng Process Process Intensif 2016;101:72–86. doi:10.1016/j.cep.2015.12.012.

[8] Gibbins J, Chalmers H. Carbon capture and storage. Energy Policy 2008;36:4317–4322.

[9] Mansouri Majoumerd M, Assadi M. Techno-economic assessment of fossil fuel power plants with CO2capture - Results of EU H2-IGCC project. Int J Hydrogen Energy 2014;39:16771–

84. doi:10.1016/j.ijhydene.2014.08.020.

[10] Davison J, Arienti S, Cotone P, Mancuso L. Co-production of hydrogen and electricity with CO2 capture. Int J Greenh Gas Control 2010;4:125–30. doi:10.1016/j.ijggc.2009.10.007.

[11] Riboldi L, Bolland O. Pressure swing adsorption for coproduction of power and ultrapure H2in an IGCC plant with CO2capture. Int J Hydrogen Energy 2016;41:10646–60. doi:10.1016/j.ijhydene.2016.04.089.

[12] Cormos C-C. Assessment of hydrogen and electricity co-production schemes based on gasification process with carbon capture and storage. Int J Hydrogen Energy 2009;34:6065–77. doi:10.1016/J.IJHYDENE.2009.05.054.

[13] Al-Mufachi NA, Rees NV, Steinberger-Wilkens R. Hydrogen selective membranes: A review of palladium-based dense metal membranes. Renew Sustain Energy Rev 2015;47:540–51. doi:10.1016/J.RSER.2015.03.026.

[14] Li H, Pieterse JAZ, Dijkstra JW, Boon J, Van Den Brink RW, Jansen D. Bench-scale WGS membrane reactor for CO2capture with co-production of H2. Int J Hydrogen Energy 2012;37:4139–43. doi:10.1016/j.ijhydene.2011.11.135.

[15] Gallucci F, Fernandez E, Corengia P, van Sint Annaland M. Recent advances on membranes and membrane reactors for hydrogen production. Chem Eng Sci 2013;92:40–66. doi:10.1016/J.CES.2013.01.008.

[16] Fan L, Li F, Ramkumar S. Utilization of chemical looping strategy in coal gasification processes 2008;6:131–42. doi:10.1016/j.partic.2008.03.005.

[17] Aziz M, Bagja F, Kurniawan W. Clean Co-production of H 2 and power from low rank coal. Energy 2016;116:489–97. doi:10.1016/j.energy.2016.09.135.

[18] Aziz M, Zaini IN, Oda T, Morihara A, Kashiwagi T. Energy conservative brown coal conversion to hydrogen and power based on enhanced process integration: Integrated drying, coal direct chemical looping, combined cycle and hydrogenation. Int J Hydrogen Energy 2017;42:2904–13. doi:10.1016/J.IJHYDENE.2016.10.060.

[19] Chen S, Hu J, Xiang W. Process integration of coal fueled chemical looping hydrogen generation with SOFC for power production and CO 2 capture. Int J Hydrogen Energy 2017;42:28732–46. doi:10.1016/j.ijhydene.2017.09.156.

[20] Li F, Zeng L, Fan LS. Techno-economic analysis of coal-based hydrogen and electricity cogeneration processes with CO2 capture. Ind Eng Chem Res 2010;49:11018–28. doi:10.1021/ie100568z.

[21] Koc R, Kazantzis NK, Nuttall WJ, Ma YH. Economic assessment of inherently safe membrane reactor technology options integrated into IGCC power plants. Process Saf Environ Prot

2012;90:436–50. doi:10.1016/j.psep.2012.07.004.

[22] Gazzani M, Turi DM, Manzolini G. Techno-economic assessment of hydrogen selective membranes for CO2 capture in integrated gasification combined cycle. Int J Greenh Gas Control 2014;20:293–309. doi:10.1016/J.IJGGC.2013.11.006.

[23] Gazzani M, Turi DM, Ghoniem AF, Macchi E, Manzolini G. Techno-economic assessment of two novel feeding systems for a dry-feed gasifier in an IGCC plant with Pd-membranes for CO2 capture. Int J Greenh Gas Control 2014;25:62–78. doi:10.1016/J.IJGGC.2014.03.011.

[24] Sofia D, Coca Llano P, Giuliano A, Iborra Hernández M, García Peña F, Barletta D. Co-gasification of coal-petcoke and biomass in the Puertollano IGCC power plant. Chem Eng Res Des 2014;92:1428–40. doi:10.1016/j.cherd.2013.11.019.

[25] Sofia D, Giuliano A, Barletta D. Techno-economic assessment of co-gasification of coal-petcoke and biomass in IGCC power plants. Chem Eng Trans 2013;32. doi:10.3303/CET1332206.

[26] Sofia D, Giuliano A, Poletto M, Barletta D. Techno-economic analysis of power and hydrogen co-production by an IGCC plant with CO2 capture based on membrane technology. Comput Aided Chem Eng 2015;37:1373–8. doi:10.1016/B978-0-444-63577-8.50074-7.

[27] Piemonte V, De Falco M, Favetta B, Basile A. Counter-current membrane reactor for WGS process: Membrane design. Int J Hydrogen Energy 2010;35:12609–17. doi:10.1016/j.ijhydene.2010.07.158.

[28] Hla SS, Park D, Duffy GJ, Edwards JH, Roberts DG, Ilyushechkin A, et al. Kinetics of high-temperature water-gas shift reaction over two iron-based commercial catalysts using simulated coal-derived syngases. Chem Eng J 2009;146:148–54. doi:10.1016/j.cej.2008.09.023.

[29] Choi Y, Stenger HG. Water gas shift reaction kinetics and reactor modeling for fuel cell grade hydrogen. J Power Sources 2003;124:432–9. doi:10.1016/S0378-7753(03)00614-1.

[30] Padurean A, Cormos CC, Agachi PS. Pre-combustion carbon dioxide capture by gas-liquid absorption for Integrated Gasification Combined Cycle power plants. Int J Greenh Gas Control 2012;7:1–11. doi:10.1016/j.ijggc.2011.12.007.

[31] You YW, Lee DG, Yoon KY, Moon DK, Kim SM, Lee CH. H2PSA purifier for CO removal from hydrogen mixtures. Int J Hydrogen Energy 2012;37:18175–86. doi:10.1016/j.ijhydene.2012.09.044.

[32] Liu PKT, Sahimi M, Tsotsis TT. Process intensification in hydrogen production from coal and biomass via the use of membrane-based reactive separations. Curr Opin Chem Eng 2012;1:342–51. doi:10.1016/j.coche.2012.06.001.

[33] Cormos CC. Evaluation of energy integration aspects for IGCC-based hydrogen and electricity

co-production with carbon capture and storage. Int J Hydrogen Energy 2010;35:7485–97. doi:10.1016/j.ijhydene.2010.04.160.

[34] Viviente JL, Meléndez J, Pacheco Tanaka DA, Gallucci F, Spallina V, Manzolini G, et al. Advanced m-CHP fuel cell system based on a novel bio-ethanol fluidized bed membrane reformer. Int J Hydrogen Energy 2017;42:13970–87. doi:10.1016/j.ijhydene.2017.03.162.

[35] Casero P, Coca P, García-Peña F, Hervás N. Case Study. Integr. Gasif. Comb. Cycle Technol., Elsevier; 2017, p. 753–75. doi:10.1016/B978-0-08-100167-7.00019-6.

[36] Cormos CC, Cormos AM. Assessment of calcium-based chemical looping options for gasification power plants. Int J Hydrogen Energy 2013;38:2306–17. doi:10.1016/j.ijhydene.2012.11.128.

[37] Grainger D, Hägg MB. Techno-economic evaluation of a PVAm CO2-selective membrane in an IGCC power plant with CO2 capture. Fuel 2008;87:14–24. doi:10.1016/j.fuel.2007.03.042.

[38] Seider WD, Lewin DR, Seader DJ, Widagdo S, Gani R, Ng KM. Product and Process Design Principles: Synthesis, Analysis and Evaluation, 4th Edition. 4th ed. New York: Wiley; 2016.

[39] Andersen MS. Europe's experience with carbon-energy taxation. SAPIENS 32 2010.

[40] Helmi A, Gallucci F, Van Sint Annaland M. Resource scarcity in palladium membrane applications for carbon capture in integrated gasification combined cycle units. Int J Hydrogen Energy 2014;39:10498–506. doi:10.1016/j.ijhydene.2014.05.009.

[41] Alique D, Martinez-Diaz D, Sanz R, Calles J. Review of Supported Pd-Based Membranes Preparation by Electroless Plating for Ultra-Pure Hydrogen Production. Membranes (Basel) 2018;8:5. doi:10.3390/membranes8010005.

[42] Satyapal S. 2009 Annual Merit Review and Peer Evaluation Report. Arlington, Virginia: 2009.